A Gut Microbial Peptide and Molecular Mimicry in the Pathogenesis of Type 1 Diabetes

Khyati Girdhar[1], Qian Huang[1], I-Ting Chow[2], Claudia Brady[1], Amol Raisingani[1], Patrick Autissier[1], Mark A. Atkinson[3,4], William W. Kwok[2], C. Ronald Kahn[5], Emrah Altindis[1]*

[1] Boston College Biology Department, Higgins Hall, 140 Commonwealth Avenue Chestnut Hill, MA 02467, USA

[2] Benaroya Research Institute at Virginia Mason, Seattle, WA 98101, USA

[3] Department of Pathology, Immunology and Laboratory Medicine, College of Medicine, University of Florida Diabetes Institute, Gainesville, FL 32610-3633, USA

[4] Department of Pediatrics, College of Medicine, University of Florida Diabetes Institute, Gainesville, FL 32610-3633, USA

[5] Joslin Diabetes Center, Harvard Medical School, Boston, MA, 02215, USA

***Corresponding Author:** Emrah Altindis, Boston College Biology Department, Higgins Hall, 140 Commonwealth Avenue Chestnut Hill, MA 02467. E-mail: altindis@bc.edu

ABSTRACT

Type 1 Diabetes (T1D) is an autoimmune disease characterized by the destruction of pancreatic β-cells. One of the earliest aspects of this process is development of autoantibodies and T-cells directed at an epitope in the B-chain of insulin (insB:9-23). Analysis of microbial protein sequences with homology to insB:9-23 sequence revealed 17 peptides showing >50% identity to insB:9-23. Of these, one peptide, found in the normal human gut commensal *Parabacteroides distasonis*, activated both human T cell clones from T1D patients and T-cell hybridomas from non-obese diabetic (NOD) mice specific to insB:9-23. Immunization of NOD mice with *P. distasonis* insB:9-23 peptide mimic or insB:9-23 peptide verified immune cross-reactivity. Colonization of female NOD mice with *P. distasonis* accelerated the development of T1D, increasing macrophages, dendritic cells and destructive CD8+ T-cells, while decreasing FoxP3+ regulatory T-cells. Western blot analysis identified *P. distasonis* reacting antibodies in sera of NOD mice colonized with *P. distasonis* and human T1D patients. Furthermore, adoptive transfer of splenocytes from *P. distasonis* treated mice to NOD/SCID mice enhanced disease phenotype in the recipients. Finally, analysis of human infant gut microbiome data revealed that exposure of infants to *P. distasonis* may modulate disease pathogenesis. Taken together, these data demonstrate the potential role for an insB:9-23-mimimetic peptide from gut microbiota as a molecular trigger or modifier of T1D pathogenesis.

43 **SIGNIFICANCE STATEMENT**

44 In Type 1 diabetes (T1D), immune cells destroy pancreatic β-cells. The trigger of this
45 response, however, is unknown. Some sequences (epitopes) in the insulin molecule form a major
46 target for this autoimmune response. We have identified a sequence in a human gut bacterium that
47 can mimetic this insulin epitope. Immune cells specific to insulin cross-react with this bacterial
48 mimetic. Further, this bacterium can accelerate diabetes onset in a mouse model of T1D, inducing
49 destructive and decreasing protective immune cells. We found this mimetic in the gut of children
50 developing T1D. Furthermore, T1D patients have a stronger immune response to this bacterium
51 compared to healthy individuals. Taken together, this bacterial mimetic in human gut has the
52 potential to trigger/modify T1D onset.

53

54

55

56

57 **1. INTRODUCTION**

58 Type 1 diabetes (T1D) is an autoimmune disease characterized by selective destruction of
59 pancreatic β-cells by autoreactive T-cells(1). Genome-wide association studies (GWAS) have
60 identified 152 genetic regions that influence the risk of developing T1D(2); however, multiple
61 studies have shown that the incidence rate of T1D in children is rising at rates exceeding what can
62 be explained on a genetic basis alone(3). Indeed, even among identical twins, the concordance of
63 T1D is only 65%(4). Likewise, there is a six-fold difference in incidence of T1D in neighboring
64 regions of Karelia in Russia and Finland, despite the very similar genetic background of the
65 inhabitants(5).

66 Various environmental factors have been studied as potential modifiers or triggers of the
67 autoimmune response in T1D including diet, birth mode, infection, and antibiotics. Viral infections
68 have been suggested to play a role in T1D pathogenesis, but most of these viruses have been
69 proposed to act by direct infection of the β-cell(6). Recently, attention has been focused on the gut
70 microbiome as a potential disease modifier through its effects on metabolite composition, intestinal
71 permeability, and regulation of the immune response in subjects with T1D(7, 8). However, the
72 exact environmental modifiers and how they might affect T1D pathogenesis remain largely
73 unknown(9).

74 One of the earliest markers of T1D is the development of islet autoantibodies(10). These
75 autoantibodies target several autoantigens including insulin, glutamic acid decarboxylase (GAD),
76 insulinoma-associated autoantigen-2 (IA-2), zinc transporter-8 (ZnT8), and an islet-specific
77 glucose-6-phosphatase catalytic subunit related protein (IGRP or G6PC2)(11). Among these,
78 insulin autoantibodies (IAA) are usually the first to be detected, and insulin is the only autoantigen
79 exclusively expressed by β-cells(12). In humans, IAA may develop years before the onset of overt

80 diabetes(13) and are especially prominent in early-onset T1D(14). They also show a significant
81 correlation with the rate of progression from prediabetes to overt disease(15). More importantly,
82 insulin or insulin-derived peptides are a target of disease pathogenetic T-cells in both humans with
83 T1D and in the most established murine model, the NOD mouse. In NOD mice, over 90% of the
84 anti-insulin T-cell clones target a single 15-amino acid peptide corresponding to the insulin B-
85 chain 9-23 sequence (insB:9-23)(15). InsB:9-23 specific T-cells have also been identified in
86 islets(16) and peripheral blood lymphocytes of T1D patients(17, 18).

87 In the present study, we hypothesized that exposure to a microbial peptide that resembles
88 the insulin epitope, insB:9-23, could stimulate or modify the autoimmune response initiating
89 T1D(19). To address this hypothesis, we analyzed bacterial, viral and fungal genome databases to
90 identify microbial proteins that have >50% sequence homology to human insB:9-23. Of these, 17
91 were synthesized and tested for ability to activate insB:9-23 specific T-cells. Herein, we
92 demonstrate that one of these peptides, a peptide from the gut commensal organism
93 *Parabacteroides distasonis*, could activate both human and NOD mouse insB:9-23-specific T-
94 cells *ex-vivo* to the same extent as the human insulin B:9-23 peptide. This bacterial peptide also
95 cross-reacts with the immune cells obtained from the mice immunized with the human insB:9-23
96 peptide. Furthermore, administration of *P. distasonis* bacteria by oral gavage accelerated T1D
97 progression in NOD mice *in vivo* by stimulating innate immune cells and CD8+ T-cells and
98 decreasing regulatory T-cells. Analysis of human gut microbiota datasets from the longitudinal
99 DIABIMMUNE study revealed the presence of this bacterial peptide in children who later
100 developed autoantibodies to insulin itself. Taken together, these studies demonstrate that an insulin
101 B:9-23-like epitope in normal gut microbiota may mimic the native insulin peptide and has
102 potential to play a role in onset or progression of T1D.

103

104 **2. RESULTS**

105 **2.1 A *P. distasonis* insB:9-23-like peptide stimulates NOD mouse hybridomas and human T-**
106 **cell clones specific to insB:9-23**

107 To determine if any microbe might have DNA encoding proteins with sequences
108 resembling the dominant T-cell epitope involved in the autoimmune response to the insulin B:9-
109 23 peptide linked to T1D (SHLVEALYLVCGERG)(15-18), we used BlastP to search NCBI
110 databases for predicted proteomes of all sequenced viruses (taxid:10239), bacteria (taxid:2), and
111 fungi (taxid:4751). We identified 47 microbial peptides with over eight residues identical to the
112 insulin peptide **(Supplementary Table S1**). Among these predicted microbial peptides, we
113 selected 17 bacterial and viral peptides that contained the largest number of previously identified
114 residues in the insB:9-23 peptide critical for this interaction(18) to be synthesized (**Figure 1A**).

115 These 17 microbial insB:9-23-like peptides, as well as a negative control
116 (irrelevant/scramble) and a positive control (insB:9-23), were then tested for their ability to
117 stimulate an insB:11-23-specific human T-cell clone isolated from a T1D patient(18) (**Figure 1B**).
118 In addition, we included a second positive control, a variant of the insB:9-23 peptide in which R
119 at position 22 is substituted by E (insB:9-23R^{22E}) and which has been shown to be even more
120 potent than native insB:9-23 in stimulating insB:9-23 hybridomas from NOD mice(20) and human
121 T-cell clones(18). As expected, in the human T-cell assay, both positive controls stimulated
122 interferon-gamma (IFN-γ) secretion with insB:9-23R^{22E} being more active than the wild type
123 sequence. Among the 17 microbial peptides tested, only one could stimulate human T-cells to
124 produce the IFN-γ (**Figure 1B**). This peptide (*hprt4-18*) represents amino acids 4-18 in the N-
125 terminus of the hypoxanthine phosphoribosyltransferase (*hprt*) protein of *Parabacteriodes*
126 *distasonis* 33B and D13 strains (formerly known as *Bacteroides sp. 2_1_*33B/ *Parabacteroides*

127 *sp.* D13)(21). Interestingly, *P. distasonis* 33B and D13 are the only organisms in the NCBI dataset
128 (as of October, 2021) that possess this insB:9-23 mimic sequence in their genomes. Next, we tested
129 the same set of microbial insB:9-23-like peptides and controls on NOD IIT-3 T-cell hybridomas,
130 previously shown to recognize the insB:9-23 epitope(22). In this assay, C3g7 cells that have high
131 expression of MHC-II I-A^{g7} were used as antigen-presenting cells (APCs) and treated with each
132 peptide at concentrations from 0.01 to 10μM. Co-culturing of these cells with IIT-3 T-cell
133 hybridomas stimulated interleukin-2 (IL-2) secretion only in presence of insB:9-23 and the *hprt4-*
134 *18* peptide, and produced similar dose-response curves, with the bacterial peptide being only
135 slightly less potent **(Figure 1C).** Thus, both human T-cell clones and NOD mouse T-cell
136 hybridomas specific to insB:9-23 were reactive to *hprt4-18*, raising the possibility that *hprt4-18*
137 may have the potential to modulate the development of T1D.
138

139 **2.2 *P. distasonis hprt4-18* peptide stimulates a T-cell response to insB:9-23 in vivo**

140 To further explore the cross-reactivity of the microbial and insulin-derived peptide
141 sequences, NOD mice were immunized with either insB:9-23 peptide or the *hprt4-18* peptide in
142 Complete Freund's Adjuvant (CFA). After 7 days, lymphocytes were isolated from the popliteal
143 lymph nodes and stimulated with either insB:9-23, *hprt4-18* or control peptides. T-cell activation
144 was assessed using an enzyme-linked immunospot (ELISpot) assay. Consistent with the in-vitro
145 results above, lymphocytes from mice immunized with the *hprt4-18* peptide exhibited a strong
146 immune response to both *hprt4-18* peptide and insB:9-23 as measured by IFNγ and IL-2 secretion
147 (**Figure 1D &1E**). Conversely, lymphocytes from mice immunized with insB:9-23 peptide
148 showed a strong response to both insB:9-23 peptide and the microbial *hprt4-18* peptide (**Figure**
149 **1F & 1G**). Taken together with the assays using the hybridoma T-cell lines, these data indicate

150 that the microbial peptide *hprt4-18* strongly cross-react with the recognition and signaling
151 machinery for human insB:9-23 in stimulating an immune response.
152
153 **2.2 *P. distasonis* colonization accelerates diabetes onset in NOD mice**
154 Based on this cross-reactivity, we hypothesized that *P. distasonis* colonization and
155 potential exposure to the microbial *hprt4-18* peptide could trigger and/or modify the immune
156 response and stimulate autoimmunity in NOD mice. To test this hypothesis, both male and female
157 NOD mice were orally gavaged with a saline suspension of *P. distasonis* (10^8 CFU/mouse/day) or
158 saline itself daily, starting at 4 weeks of age (i.e., after weaning) and followed for 30 weeks (**Figure**
159 **2A**, n=40/group). Two weeks after the last oral gavage, qPCR using fecal DNA samples revealed
160 significant levels of *P. distasonis* in the feces of the treated mice, whereas neither male nor female
161 control NOD mice housed under specific pathogen-free (SPF) conditions had *P. distasonis* in their
162 gut microbiome (**Figure 2B**). At 12 weeks of age, when mice are in the pre-diabetic stage, five
163 mice from each group were randomly selected and examined histologically for insulitis. In the *P.*
164 *distasonis* colonized female NOD mice there was more than 2-fold increase in severe insulitis
165 scores as compared to controls (**representative images in 2C, Figure 2D**). Consistent with the
166 increase in insulitis, female NOD mice subjected to *P. distasonis* colonization showed significantly
167 accelerated onset of T1D with only 19.5% disease-free in the *P. distasonis* colonized group versus
168 42% disease-free in the control group (**Figure 2E**). This effect was specific to the female mice,
169 with no differences in insulitis scores or T1D incidence in male NOD mice with *P. distasonis*
170 colonization (**Supplementary Figure S1A-B)**.

171 To determine whether *P. distasonis* colonization stimulates an immune response against
172 the bacterium, we performed Western blot analysis in which *P. distasonis* cellular protein lysates

173 were resolved on SDS-PAGE, transferred to PVDF membranes, then probed using serum samples
174 from 12-week-old *P. distasonis* colonized or control NOD mice. *P. distasonis* colonization of the
175 NOD mice gut stimulated an antibody response to multiple bacterial proteins in both female and
176 male NOD mice (**Figure 2F, Supplementary Figure S1C**). This response was specific; Western
177 blots using protein lysates from *Bacteroides fragilis*, another gut microbe that has been shown to
178 have immunomodulatory effects in NOD mice(23), produced only a weak humoral immune
179 response in both the saline and *P. distasonis* treated groups **(Supplementary Figure S1D-E**).
180 Importantly, serum LPS levels were not significantly different between the groups, indicating that
181 the *P. distasonis* humoral response was not the result from of general gut barrier dysfunction
182 stimulated by bacterial colonization **(Supplementary Figure S1F**).

183 To determine whether there is a similar enrichment in the humoral immune responses
184 against *P. distasonis* occurs in humans with T1D, Western blot analysis was performed using
185 serum samples from 12 T1D patients (median age 17.5, median disease duration 8 years, males)
186 with age, sex and ethnicity matched controls. As shown in **Supplementary Figure S1G,** there was
187 a very weak humoral response against *P. distasonis* in healthy subjects, strong reactivity was
188 observed in seven out of 12 T1D patients. Thus, consistent with our findings in NOD mice, at least
189 a subset of T1D patients appear to have a humoral immune response to *P. distasonis* proteins.

190 **2.3 Adoptive transfer of splenocytes enhances T1D onset in NOD/SCID mice**

191 To determine if the enhanced development of T1D in the NOD receiving *P. distasonis*
192 colonized mice was T-cell mediated, we performed an adoptive transfer experiment using
193 immunodeficient NOD/SCID mice, which lack functional B and T cells, as recipients(24). To this
194 end, a new cohort of NOD mice was orally gavaged with *P. distasonis* or saline (n=15-20/group)

195 as described above. At week 15, these mice were sacrificed, and $5x10^6$ splenocytes were
196 transferred from individual NOD diabetes-free donors to 9-week-old NOD/SCID recipients (1:1
197 ratio, sex-matched) after which the recipients were followed for 10 weeks **(Supplementary Figure**
198 **S2A**). Consistent with the effect of *P. distasonis* colonization on spontaneous T1D in NOD mice
199 (**Figure 2G**), female NOD/SCID mice that received splenocytes from the *P. distasonis* treated
200 group developed T1D at a higher rate than those receiving splenocytes from control NOD mice.
201 Thus, at 10 weeks following transfer, 62.5% of recipients of receiving control splenocytes
202 remained disease free, and this was decreased to 31% in mice receiving splenocytes from *P.*
203 *distasonis* colonized NOD donors (**Figure 2G)**. Hence, the immune response stimulated by *P.*
204 *distasonis* in female NOD mice was sufficient to accelerate T1D in NOD/SCID mice.

205 **2.5 *P. distasonis* colonization increases CD8+ T-cells and decreases Foxp3+ regulatory T cells**
206 **in the splenocytes of female NOD mice.**

207 To determine the effects of *P. distasonis* treatment on NOD mice immune cell composition,
208 a new cohort of 12-week-of age NOD mice was orally gavaged with either *P. distasonis* or saline,
209 and the T-cell populations in splenocytes and pancreatic lymph nodes (PLNs) assessed by flow
210 cytometry. The gating strategy for different T-cell subsets and innate immune cells are described
211 in **Supplementary Figure S3A & B**. We found that in the spleens of *P. distasonis* colonized NOD
212 mice there was a significant 31% increase in CD8+ T-cells**,** leading to a 30 % decrease in the
213 CD4/CD8 ratio **(Figure 3A & 3B)**. PLN cells isolated from the *P. distasonis* colonized mice
214 showed similar trends in CD4+ T-cells, CD8+ T-cells, and CD4/CD8 ratio, but these did not quite
215 reach statistical significance **(Supplementary Figure S4A & S4B)**. Using FACS analysis, we also
216 determined the various subsets of cells including naive cells ($CD44^{lo}$ $CD62L^{hi}$), effector memory
217 cells (T_{EM}, ($CD44^{hi}$ $CD62L^{lo}$), and, central memory cells (T_{CM}, $CD62L^{hi}$ $CD44^{hi}$) in the

218 TCRβ+/CD8+/CD4+ cell population in both the spleen and PLN (**Figure 3C-3F**). This revealed a
219 significant increase in the TCRβ+/CD8+/CD4+ naive T-cell population (**Figure 3D, 3E**) and a
220 decrease in T_{EM} $CD4^+$ T-cells in splenocytes (**Figure 3C-3F**) but no alterations in TCRβ+/CD4+
221 naive cells in PLNs of *P. distasonis* colonized mice **(Supplementary Figure S4C-S4F**). There
222 was also a two-fold increase in the naive cell population in both CD4+ and CD8+ T-cells in spleen
223 (**Figure 3E & F**) and in the CD8+ naive cell population in PLNs **(Supplementary Figure S4F**).
224 There were no differences in the central memory cells and effector memory cell populations in
225 TCRβ+/CD8+ cells in splenocytes (**Figure 3D & 3F**) or in TCRβ+/CD8+/CD4+ cells in PLNs
226 **(Supplementary Figure S4D-S4F**).
227 T-regulatory cells (Treg) play a key role in modulating T1D autoimmunity by suppressing
228 self-reactive T-cell proliferation(25). This is modulated by Forkhead box protein P3 (Foxp3)
229 expression and interleukin 10 (IL-10) secretion. It has previously been shown that CD4+ CD25+
230 CD44+ Treg cells positively correlate with Foxp3 expression and production of IL-10(26). We
231 found a 15 % decrease of CD4+ CD25+CD44+ Treg cells in both splenocytes (**Figure 3G & 3H**)
232 and PLN cells **(Supplementary Figure S4G & S4H**) and a 1.6-fold increase in the total CD4+
233 CD25+ PLN cell population **(Supplementary Figure S4H)** of *P. distasonis* colonized mice. While
234 there were no differences in other cell subsets **(Figure 3H).** In the CD4+ T-cell population, the
235 percentage of Foxp3+ cells were significantly decreased in the splenocytes and PLNs of *P.*
236 *distasonis* colonized NOD mice by 21% and 17.8%, respectively (**Figures 4A, 4B & S5A,**
237 **representative images**). There was no difference in the pancreas and spleen weight or in the total
238 number of the spleen and PLN cells between *P. distasonis* colonized mice and the control mice
239 (**Supplementary Figure 5B).** Thus, *P. distasonis* colonization decreases anti-inflammatory CD4+

240 CD25+ CD44+ and Foxp3+ Tregs and increase inflammatory CD8+ T-cells in splenocytes and
241 PLNs, which could contribute to the enhancement of T1D in female NOD mice.

242 **2.6 *P. distasonis* colonization in female NOD mice increases dendritic cells and macrophages**
243 **in the splenocytes**

244 To further explore the mechanisms that lead to an increase in CD8+ T-cells in *P. distasonis*
245 colonized NOD female mice, we assessed the number of the APCs in spleens and PLNs. CD11c+
246 CD11b+ dendritic cells and F4/80+ macrophages play an essential role in accelerating diabetes in
247 NOD mice(27, 28). FACS analysis revealed a 1.5-fold increase in CD11b+ CD11c+ dendritic cells
248 and a 1.6-fold increase in F4/80+ macrophages in the splenocytes of *P. distasonis* colonized mice
249 (**Figure 4C-F**), with no significant differences in dendritic cells in PLNs **(Supplementary Figure**
250 **S5D-S5G**). Moreover, CD11c+ CD11b- dendritic cells(29) increased 1.8-fold in the spleen of *P.*
251 *distasonis* colonized mice (**Figure 4D**). There was also a 1.3-fold increase in circulatory
252 macrophages ($SSC^{lo}Ly6C^{hi}$ cells), while there was no change in the number of residential
253 macrophages ($SSC^{lo}Ly6C^{lo}$) in this population **(Figure 4G)**. However, there was 7-fold increase
254 in F4/80+ macrophage population in PLN in *P. distasonis* colonized mice **(Supplementary Figure**
255 **S5G**). These findings are consistent with previous studies demonstrating a role of CD11c+
256 CD11b+ dendritic cells and F4/80+ macrophages in accelerating diabetes in NOD mice(27, 28)
257 and demonstrated that *P. distasonis* colonization can stimulate both innate and adaptive immune
258 responses.

259

260 **2.7 Critical timing of *P. distasonis hprt4-18* exposure in gut microbiome samples of children**
261 **developing T1D in early life.**

262 To investigate the potential role for the *P. distasonis* insB:9-23 mimetic peptide in human
263 T1D, we reanalyzed human gut microbiome data from the DIABIMMUNE study [57] using shotgun
264 metagenomic sequencing performed on stool samples collected monthly from infants 0-3 years of
265 age who were genetically predisposed to T1D living in Finland, Russia and Estonia and correlated
266 this with development of islet autoantibodies, i.e., seroconversion(30). Using the metagenomic
267 data of this study, we searched for the specific DNA sequences encoding the *P. distasonis hprt4-*
268 *18* peptide. We found that in the children who remained negative for autoantibody markers for
269 T1D, sequences encoding *P. distasonis hprt4-18* were detectable in 20-40% patients with no
270 significant change between ages 0 to 3. By comparison, in children who later became autoantibody
271 positive, *hprt4-18* encoding sequences were absent in the first year of life, began to appear by age
272 2 and then were found in 60% of the children by age 3 (**Figure 5A**).

273 The exact frequency and timing of appearance of the *hprt4-18* sequence in the microbiome
274 varied by country. Thus, in subjects from Estonia (14 of 74 infants) and Russia (4 of 74 infants),
275 for those who became seropositive, we did not find the *hprt4-18* sequence in their gut microbiota
276 during the first year of life, but was found in 100% of subjects who developed autoantibodies by
277 the age of 2 or 3 (**Figure 5B**). In contrast, this sequence was found in 15-40% of the seronegative
278 infants throughout this time period. Interestingly, while children in Finland who were seronegative
279 has similar prevalence of the microbial sequence as those in Estonia and Russia, infants who
280 became seropositive in Finland (16 of 74 infants) had no detectable *hprt4-18* sequences during the
281 first three years of life (**Figure 5B**). These results suggest that a delayed exposure to the *P.*
282 *distasonis hprt4-18* peptide, i.e., after the first year of life, may be able to trigger or potentiate an
283 autoimmune response that leads to development of T1D in genetically susceptible individuals.

284 This is also consistent with our findings in NOD mice where colonization of the female NOD mice
285 with *P. distasonis* after weaning accelerated diabetes development.

286 **3. DISCUSSION**

287 Despite major increases in our understanding of the role of autoimmunity in pathogenesis
288 of T1D, the triggering events which lead to disease development remain poorly understood. It is
289 well known that an important component of the early autoimmune response in individuals who
290 ultimately develop T1D is the development of autoantibodies and T-cell reactivity to islet proteins,
291 especially insulin. While there are multiple potential epitopes, the dominant sequence within the
292 insulin molecule to which reactivity occurs is a sequence in the B-chain involving amino acids 9-
293 23(14). This B:9-23 peptide (SHLVEALYLVCGERG) can bind to DQ8 molecules utilizing three
294 different registers, with the amino acid V at position 12, E at position 13 or A at position 14(31).
295 It has been shown that a R→E substitution at position 22 of the B:9-23 peptide creates an even
296 more potent agonist for activating B:9-23 T cell clones, implicating the A at position 14 as the p1
297 anchor(18).

298 In this study, we have investigated the potential role of molecular mimicry as a link
299 between microbial flora and this component of T1D development. Molecular mimicry mechanisms
300 are based on the degeneracy of T-cell recognition(32, 33) and can be either pathogenic(34) or
301 protective(35). While molecular mimicry has long been postulated as a potential factor in
302 autoimmune diseases, including T1D (36, 37), progress in this area has been limited due to a lack
303 of identification of microbial sequences which might trigger this response(38). In the current study,
304 taking advantage of the growing genome databases for microbes in the environment, we have
305 identified 47 microbial peptides with high sequence homology to insB:9-23. We demonstrate that

306 of these, a peptide with the sequence of *hprt4-18* from *P. distasonis,* can be recognized by and
307 activate both murine and human T-cells known to respond to insB:9-23 and can cross-stimulate an
308 immune response to the insB:9-23 peptide in mice. Moreover, exposure of NOD mice to *P.*
309 *distasonis* in the gut microbiome during early life results in increased insulitis and accelerates
310 diabetes onset. This pathogenic effect is mediated by CD8+ T splenocytes, as evidenced by the
311 ability to adoptively transfer this increase in diabetes risk to female NOD/SCID mice.

312 Microbiota and gut microbiota in particular have been shown to play a role in modulating
313 T1D onset in NOD mice(7, 39-41), but previous reports have identified primarily protective
314 effects, and most through somewhat non-specific mechanisms. For example, NOD mice reared in
315 germ-free environments have higher rates of development of diabetes than those raised in
316 conventional facilities(40). In terms of protective effects of some specific bacterial species, the
317 presence of segmented filamentous bacteria in the gut correlates with diabetes protection in NOD
318 female mice, which normally have a high incidence of disease(42). Likewise, female NOD mice
319 colonized at 3-10 weeks of age with *Akkermensia muciniphila* show delayed diabetes
320 development(43), and oral administration of heat-killed *B. fragilis* has been shown to suppress
321 autoimmunity in NOD mice when administered under conditions which induce increased gut
322 permeability(23). Since literally hundreds of treatments have been shown to decrease development
323 of diabetes in NOD mice (44, 45), however, the specificity of these effects has been
324 questioned(46). By contrast, in the present study we show that exposure to *P. distasonis* can
325 accelerate disease development in NOD mice and that a specific peptide encoded in their genome,
326 *hprt4-18*, can serve as a mimic of the major insulin auto-epitope at position B9-23. This peptide
327 and the insulin peptide can also stimulate a bidirectional cross-reactive immune response, proving
328 its nature as a molecular mimic.

329 In addition to the immunologic cross-reactivity, our study also provides some insight
330 into the mechanisms of immune cell regulation by this bacterium. Thus, colonization of NOD mice
331 with *P. distasonis* increases the CD8+ T-cell population and decreases the CD4/CD8 T-cell ratio.
332 A reduction in this ratio has been previously shown to be associated with increased T1D in
333 humans(47). G9C8 CD8+ T-cell clones originally isolated from the islets of young NOD mice
334 cells are activated by an insB:15-23 peptide, i.e., the C-terminal fragment of the insB:9-23 peptide,
335 and this accelerates diabetes when adoptively transferred in NOD/SCID mice, even in the absence
336 of CD4+ T-cells(48, 49). Wong *et al.* showed that cross presentation of insulin by dendritic cells
337 can stimulate G9C8 T-cell clones, and both insulin and the insB:15-23 peptide can stimulate
338 proliferation of the naive cell phenotype in NOD mice (48). The *P. distasonis* sequence is identical
339 to this peptide in 6 of its 9 residues. We also observed that *P. distasonis* colonization in NOD mice
340 decreased Foxp3+ Treg cells in spleen and PLNs. This effect on Foxp3+ Treg cells is particularly
341 interesting because Foxp3+ Treg cells are dysregulated in newly diagnosed T1D patients(50) and
342 increasing Foxp3+ Treg cells in NOD mice can delay the onset of diabetes in NOD mice(25, 51).

343 A plethora of human gut microbiome studies have demonstrated that the composition of
344 gut microbiota in patients with autoimmune diseases, including multiple sclerosis(52), systemic
345 lupus erythematosus, anti-phospholipid syndrome(53), Crohn's disease(54-56), ulcerative
346 colitis(57), inflammatory bowel diseases(58, 59), and celiac disease(60) are significantly different
347 from those in healthy controls. Although the methodologies and conclusions differ in studies of
348 microbiota from subjects with or at-risk for T1D(8, 30, 61), most show that the diversity of gut
349 microbiota is decreased in T1D patients with increased prevalence of *Bacteroidetes* species. This
350 is also associated with an altered serum metabolomic profile compared to healthy controls(7).
351 While most of these studies have not been able to define any mechanism by which this might relate

352 to disease development, data in the DIABIMMUNE study[57] has suggested that the higher T1D
353 rates in Finnish Karelia and Estonia compared to Russian Karelia may in part be related to an
354 action of different lipopolysaccharides (LPS) present in the gut microbiota on the immune
355 response.

356 The Environmental Determinants of Diabetes in the Young (TEDDY) study, which has
357 collected over 12,000 fecal samples from 903 children at risk for T1D in four countries, has
358 identified *Parabacteroides* as the genus most significantly associated with T1D(62). This is
359 consistent with our findings that a *P. distasonis* peptide can induce T-cells and antibodies that
360 cross-react with the major epitope in insulin involved in the autoimmune response. Reanalysis of
361 the DIABIMMUNE metagenomic data show that 100% of the children becoming seropositive for
362 autoantibodies related to T1D in Russia and Estonia have the DNA encoding the *P. distasonis*
363 hprt4-18 peptide in their gut microbiota in first 2-3 years of life compared to less than 40% of
364 children remaining seronegative. Interestingly, most of these seroconverters were negative for this
365 microbial sequence in the first year of life, suggesting the timing of exposure to this microbial
366 antigen may be important in disease development. The TEDDY study showed that human gut
367 microbiota development can be divided into three phases: a developmental phase (months 3-14),
368 a transitional phase (months 15-30), and a stable phase (months 31-46)(62). Our data suggest that
369 exposure to *P. distasonis* in the transitional phase may be critical in T1D pathogenesis. Further
370 studies will be needed to directly investigate the link between human T1D and *P. distasonis*, but
371 the cross-reactivity of the *P. distasonis hprt*4-18 peptide with insB:9-23 activated human T cell
372 clones represents a clear potential mechanism.

373 While we have focused only on insulin and the B:9-23 peptide as an antigenic determinant
374 of disease, there are clearly other epitopes recognized by both circulating and islet-infiltrating T-

375 cells in the insulin B-chain(63), A-chain(64, 65), or C-peptides(16, 66). The recent discovery that
376 hybrid insulin peptides (HIPs) may be novel epitopes formed by post-translational modifications
377 formed in the beta cell(67, 68) also opens the possibility of microbial sequences that may more
378 closely mimic these hybrid peptides. Defective ribosomal products (Drips) of insulin have also
379 been shown to lead to aberrant insulin polypeptides rendering beta cells immunogenic(69). We
380 must also keep in mind that insulin is not the only antigen to which antibodies or reactive T-cell
381 lines are formed in T1D. Other islet antigens include GAD, IA-2, and HIPs(70). Given the
382 enormous number of microbial peptides produced by the gut microbiota, we expect that other
383 microbial peptides may exist with the potential to mimic these epitopes and/or trigger related
384 autoantigen reactive T-cells. Indeed, Tai *et al.* identified a microbial peptide mimic produced by
385 *Fusobacteria* that can stimulate islet-specific glucose-6-phosphatase (IGRP) specific mouse T-
386 cells and promote diabetes development in a new Toll-like receptor (TLR) deficient ($TLR^{-/-}$) and
387 $MyD88^{-/-}$ NY8.3 NOD mouse model(71).

388 In summary, our data define a novel molecular mimicry mechanism in which a specific
389 sequence in a normal commensal gut microbe can mimic a sequence in insulin B-chain and trigger
390 or modify the immune response involved in development of T1D. This finding may provide a new
391 target for treat and a window of opportunity to prevent or delay T1D development. These data also
392 have implications for other diseases with an autoimmune component. Today, we have databases
393 with enormous amounts of microbial and microbiome sequence data, which can be leveraged to
394 address the role of molecular mimicry in the autoimmunity, not only of T1D, but also lupus
395 erythematosis(72), inflammatory cardiomyopathy(73), and multiple sclerosis(74). Our findings
396 demonstrate a new link to gut antigens and autoimmune diseases with the potential to ultimately

397 provide new tools, including vaccines, antibiotics, or probiotics for the prevention and treatment
398 of autoimmune diseases.
399
400

401 **4. MATERIAL AND METHODS**

402 **4.1 Bioinformatics**

403 A bioinformatics search was performed using NCBI BLASTp for the presence of the
404 microbial peptide sequences with homology to human insB:9-23 sequence as query against viral
405 (NCBI taxonomic ID: 10239), bacterial (NCBI taxonomic ID: 2), and fungal (NCBI taxonomic
406 ID: 10239) proteomes. The whole peptide sequence of each significant hit was compared with
407 insB:9-23 using a multiple sequence alignment program (Clustal Omega) to determine the number
408 of identical and conserved residues. This yielded the data in **Supplementary Table S1**. An
409 additional bioinformatics search was performed to determine whether *P. distasonis* peptide is
410 unique. *P. distasonis* peptide (15aa) or *P. distasonis* hypoxanthine phosphoribosyltransferase
411 *(hprt4-18)* protein sequences were used as queries and searched against BLASTp using non-
412 redundant protein sequences.

413 **4.2 Bacterial culture**

414 *Parabacteroides distasonis* D13 strain was purchased from Dr. Emma Allen-Vercoe's
415 laboratory at the University of Guelph. Dr. Allen-Vercoe's group isolated this bacterium from the
416 colon of an ulcerative colitis patient. *P. distasonis* D13 strain and *Bacteroides fragilis*
417 (ATCC® 25285) were cultured in anaerobic culture broth (Tryptic Soy Broth supplemented with
418 5 µg/ml Hemin (BD Biosciences) and 1µg/ml Vitamin K1 (VWR) at 37°C in an anaerobic chamber
419 (Coy Laboratory Product).

420 **4.3 Animals**

421 NOD/ShiLtJ (NOD) and NOD. Cg-*Pcrkdc scid*/J (NOD/SCID) mice were purchased from
422 Jackson Laboratory. Mice were maintained and bred in the Boston College Animal Care Facility.

423 The mice were maintained under specific pathogen-free conditions in a 12-hrs dark/light cycle
424 with autoclaved food, water, and bedding. All experiments complied with regulations and ethics
425 guidelines of the National Institute of Health and were approved by the IACUC of Boston College
426 (Protocol No.#B2019-003 and 2019-004). For colonization, *P. distasonis* bacteria were re-
427 suspended in saline at a concentration of 10^9 CFU/mL and oral gavaged using 22ga plastic feeding
428 tube (Instech Laboratories) (100µl/mouse, 10^8 CFU/mouse). 3-week-old NOD mice were orally
429 gavaged with *P. distasonis* D13 daily for four weeks right after weaning for 4 weeks. Control
430 groups were gavaged with sterile saline.

431 To determine colonization, the DNA was extracted from 100 mg mouse fecal samples (9-
432 week-old, 2 weeks after final oral gavage treatment) using QIAamp PowerFecal Pro DNA kit
433 (Qiagen) following the manufacturer's instruction. qPCR was conducted using QuantStudio 3
434 Real-Time PCR System (Applied Biosystems) with Power SYBR Green Master Mix (Applied
435 Biosystems) following manufacturer's instruction. The primers were described previously and
436 listed in Supplementary **Table S2**(75, 76). The relevant abundance of *P. distasonis* was determined
437 through being normalized with *Eubacteria.*

438 **4.4 Human T-Cell Clone Stimulation.**

439 Twenty 15-mer peptides **(Figure 1A**) used in human and mouse T-cell stimulation
440 experiments were chemically synthesized by Genscript (TFA removal, >85% purity). The peptides
441 were dissolved in DMSO at 20 mg/mL (∼12 mM). Human T-cell clone stimulation assays were
442 performed as previously described(77). Briefly, insB:11-23-specific T-cell clones were stimulated
443 in 96-well round- bottom plates with irrelevant, specific, or microbial mimotope peptides in the
444 presence of irradiated DQ8cis- or DQ8trans-expressing HEK293 cells as APCs. 50 µl of
445 supernatants from cultures of T cell clones were collected after 48 hrs of stimulation and added to

446 each well of 96-well round-bottom plates precoated with IFN-γ (clone MD-1) capturing antibodies
447 (BioLegend). After overnight incubation, bound cytokines were detected by biotinylated anti-IFN-
448 γ (clone 4s.B3) and quantified using a Victor2 D time-resolved fluorometer (Perkin Elmer). The
449 % activity was calculated by dividing the SI of mutated peptides by the SI of the wild-type peptide.
450 Experiments were performed in the presence of 1 μg/ml of anti-CD28 antibodies. Unless otherwise
451 stated, peptide concentrations were 2.5 μM.

452 **4.5 NOD mice T-cell stimulation and antigen presentation assay**

453 This experiment was performed as described previously(22). Briefly, the peptides were
454 ordered from Genscript (TFA removal, >85% purity) and dissolved in a base buffer consisting of
455 50 mM NaCl, 10 mM HEPES, pH 6.8 with 200 μM TCEP. *P. distasonis hprt4-18* peptide -
456 **(RILVELLYLVCSEYL)** was dissolved in 5% DMSO (the final DMSO concentration is less than
457 1%). The C3g7 cell line, which expresses an abundance of MHC-II I-A^{g7}, was used as APCs and
458 was treated with 1/2log dilutions of peptide (starting from 10 μM). These cells were then cultured
459 with the IIT-3 T-cell hybridomas for 18 hrs. Culture supernatants were assayed for IL-2 by
460 incubation with the CTLL-2 cell line. CTLL-2 cells are responsive to IL-2 and only actively divide
461 in the presence of IL-2. Next, CTLL cell proliferation was determined by 3H uptake (CPM) using
462 a scintillation counter.

463 **4.6 Immunization of the NOD mice**

464 The experiments were performed as described previously(78). Briefly, 13 weeks old male
465 NOD mice (n=3 mice per group) were immunized in the footpad with the either *hprt4-18* peptide
466 or insB:9-23 peptide (10 nmol/mouse). After 7 days, the draining (popliteal) lymph nodes were
467 removed and pooled for examination by ELISpot. In the ELISpot assay, node cells were recalled

468 with the various peptides to elicit either an IL-2 or IFN-γ response. Spots were analyzed by
469 Immunospot 5.0 (C.T.L.)

470 **4.7 Reanalysis of the published metagenomics data**

471 DIABIMMUNE data was downloaded with the help of Dr. Alex Kostic. The reads were
472 assembled using SPAdes as the reads were not ideal for peptide search(30) and are now available
473 at https://github.com/ablab/spades. These assembled contigs were used for a tBLASTn search to
474 identify "RILVELLYLVCSEYL" encoding sequences in these samples. The data was classified
475 based on the country and collection time of the stool samples, e.g., 0-1, 1-2, and 2-3 years.

476 **4.8 Splenocyte transplantation**

477 Splenocytes were isolated from 15 weeks donor NOD mice by filtering through a sterile
478 70 µm nylon mesh. The isolated splenocytes were incubated for 3 mins in red blood cell lysis with
479 ACK (Lonza) followed by washing with media. The isolated splenocytes were intravenously
480 injected ($5x10^7$ cells/mouse) through lateral tail vein into recipient NOD/SCID mice (9 weeks old).
481 Donor NOD mice and recipient NOD/SCID mice were sex-matched. Recipient mice were
482 monitored for diabetes by checking tail vein blood glucose levels (>250 mg/dl) twice per week.
483 The experiment terminated 10 weeks after the transplantation or unless the mice were diagnosed
484 with diabetes. Donor mice were 15-week male or female NOD mice colonized with either *P.*
485 *distasonis* or their sex-matched saline control (n=15-19).

486 **4.9 FACS and Flow Cytometry:**

487 We collected spleen and Pancreatic Lymph Nodes (PLNs) cells from saline-treated and
488 *P. distasonis* colonized female NOD mice at 12 weeks age. Single-cell suspension was obtained
489 by mechanical disruption of spleen and PLNs using an Ammonium-Chloride-Potassium (ACK)

490 lysis buffer for 5 minutes followed by filtration with a 70-µm filter. For staining of surface
491 markers, cells were incubated in fluorescently labeled antibodies **(Supplementary Table S4**) for
492 15 minutes in PBS containing 2% FBS at room temperature. Cells were then washed with 2 mL
493 of staining buffer and fixed with 1% Paraformaldehyde (PFA). For Foxp3 staining, fix and perm
494 permeabilization kit (Thermo fisher) was used as per manufacturer instruction. All the flow
495 cytometry antibodies were obtained from BioLegend, and Flow cytometry was performed using
496 BD FACSAria III sorter (BD biosciences) at the Boston College Core facility. The data was
497 analyzed using FlowJo 10.0 software. Gating strategy for the determination of different cells
498 subsets are described in supplementary **Figure S2.**

499 **4.10 Insulitis score**

500 Pancreata were isolated from *P. distasonis* colonized 12 weeks NOD mice and control mice
501 (n=5) followed by fixation with 4% paraformaldehyde overnight at 4°C. Pancreata were embedded
502 in paraffin blocks and were sectioned into 5µm thickness. To determine insulitis scores, pancreatic
503 sections were stained with hematoxylin-eosin at Harvard University BIDMC Histology Core.
504 Slides were analyzed using EVOS XL Core microscope with an LPlan PH2 10 × /0.25 and an
505 LPlan PH2 20×/0.40 objective. The pancreatic insulitis was screened and evaluated as described
506 previously(79).

507 **4.11 Western Blot analysis**

508 Protein lysate was extracted using CelLytic B Cell Lysis Reagent (Sigma) following the
509 manufacturer's instruction. Protein concentrations were determined using BCA assay
510 (ThermoFisher Scientific). 20 µg of total denatured bacterial protein was loaded into each well in
511 SDS gel. Wet transfer was performed by using PVDF membrane for 1 h at 4°C. The membrane

512 was then blocked with 5% non-fat milk in PBST. After washing, the membrane was incubated
513 with mouse serum (1: 2,500) or human serum (1: 10,000) overnight at 4°C followed by washing
514 three-time wash with PBST and incubation with secondary antibodies, sheep anti-mouse IgG
515 antibody (1:3000, Millipore) or goat anti-human IgG antibody (1:3000, SantaCruz) for 1 h at room
516 temperature. The membrane was washed and developed with chemiluminescent substrate ECL
517 (ThermoFisher Scientific).

518 **4.12 Endotoxin ELISA**

519 12-weeks old NOD mice serum was collected and stored at −80 °C until use. Serum
520 endotoxin levels were measured using a Pierce Chromogenic Endotoxin Quant Kit (ThermoFisher
521 Scientific) following the manufacturers' instructions.

522 4.13. **Human Plasma Samples**

523 Peripheral blood was collected from living subjects following the provision of written
524 informed consent (and assent in the case of minors) in accordance with IRB approved protocols
525 (University of Florida IRB# 201400703) and the Declaration of Helsinki. The patient
526 demographics outlined in **Supplementary Table 3**.

527 **4.14 Statistics**

528 Data are presented as the mean ± SEM. Survival curves were analyzed by a log-rank
529 (Mantel-cox) test. Statistical significance was evaluated using unpaired two-tailed Student's *t*-test
530 for two-group comparison or ANOVA, followed by Dunnet's or Šidák's multiple comparisons
531 tests whichever was recommended. A *p-value* of less than *0.05* was considered significant (*) at
532 the confidence interval of 95%.

533 **Acknowledgements**

534 We first want to thank Prof. Emil Unanue and Dr. Anthony Vomund (University of
535 Washington, St. Louis) for testing microbial insulins on T-cell hybridomas, immunization
536 experiments, and their help to interpret the data. Thanks to Jonathan Dreyfuss and Hui Pan (Joslin
537 Bioinformatics Core) for bioinformatics analysis. Thanks to Babak Momeni (Boston College) for
538 sharing his laboratory's anaerobic chamber. We thank Bret Judson and the Boston College
539 Imaging Core for infrastructure and support. We acknowledge our undergraduate students Tu
540 Tran, Ruixu Huang, David Kim, Scott Hsu, Kaan Sevgi and Maximilian Figura and Typhania
541 Zanou for their help with the microscopy work and the animal experiments. Thanks to Nancy
542 McGilloway and Todd Gaines for their support in the Boston College Animal Care Facility. We
543 thank Alex Kostic, Tao Xu, Thomas Serwold, and Shio Kobayashi (Joslin Diabetes Center) for
544 valuable Discussion.

545 **Funding:** This work was supported by (i) National Institutes of Health Grants 1K01DK117967-
546 01 (to E.A.), R01DK031036 and R01121967 (to C.R.K.) and NIH P01 AI042288 (to MAA) and
547 (ii) The G. Harold and Leila Y. Mathers Charitable Foundation Research Grant MF-1905-00311
548 (to E.A).

549 **Author contributions:** K.G assisted with NOD mice experiments, NOD mice colonization
550 followed by FACS staining, data analysis and writing the manuscript. Q.H assisted with NOD
551 mice experiments; NOD mice oral gavage, splenocytes transfer, qPCR, and Western blot analysis
552 using mice serum. I.C and W.K assisted with the experiments using NOD mice T-cell clones. C.B
553 and A.R assisted with oral gavage experiments and following the diabetes onset in NOD mice. P.A
554 assisted with FACS facilities and instrument handling. CRK assisted with research design and data

555 analysis. All authors assisted with the analysis of the data. E.A completed bioinformatics analysis
556 for the mimic identification, supervised the project, analyzed the data and wrote the paper.

557 **Competing Interests:** The authors do not have any conflict of interest related to this study.

558 **Data and materials availability:** Because the DIABIMMUE study metagenomics sequencing
559 reads were not ideal for a peptide search, we first assembled the reads using SPAdes (11), and they
560 are available at https://github.com/ablab/spades.

561 **REFERENCES:**

562 1. Pugliese A (2017) Autoreactive T cells in type 1 diabetes. *J Clin Invest* 127(8):2881-2891.
563 2. Robertson CC*, et al.* (2021) Fine-mapping, trans-ancestral and genomic analyses identify
564 causal variants, cells, genes and drug targets for type 1 diabetes. *Nat Genet* 53(7):962-971.
565 3. Mayer-Davis EJ*, et al.* (2017) Incidence Trends of Type 1 and Type 2 Diabetes among
566 Youths, 2002-2012. *N Engl J Med* 376(15):1419-1429.
567 4. Redondo MJ, Jeffrey J, Fain PR, Eisenbarth GS, & Orban T (2008) Concordance for islet
568 autoimmunity among monozygotic twins. *N Engl J Med* 359(26):2849-2850.
569 5. Kondrashova A*, et al.* (2005) A six-fold gradient in the incidence of type 1 diabetes at the
570 eastern border of Finland. *Ann Med* 37(1):67-72.
571 6. Coppieters KT, Boettler T, & von Herrath M (2012) Virus infections in type 1 diabetes.
572 *Cold Spring Harb Perspect Med* 2(1):a007682.
573 7. Dedrick S*, et al.* (2020) The Role of Gut Microbiota and Environmental Factors in Type 1
574 Diabetes Pathogenesis. *Front Endocrinol (Lausanne)* 11:78.
575 8. Kostic AD*, et al.* (2015) The dynamics of the human infant gut microbiome in development
576 and in progression toward type 1 diabetes. *Cell Host Microbe* 17(2):260-273.
577 9. Boljat A*, et al.* (2017) Environmental Risk Factors for Type 1 Diabetes Mellitus
578 Development. *Exp Clin Endocrinol Diabetes* 125(8):563-570.
579 10. Ziegler AG*, et al.* (2013) Seroconversion to multiple islet autoantibodies and risk of
580 progression to diabetes in children. *JAMA* 309(23):2473-2479.
581 11. Atkinson MA, Eisenbarth GS, & Michels AW (2014) Type 1 diabetes. *Lancet*
582 383(9911):69-82.
583 12. Zhang L, Nakayama M, & Eisenbarth GS (2008) Insulin as an autoantigen in NOD/human
584 diabetes. *Curr Opin Immunol* 20(1):111-118.
585 13. Palmer JP, Asplin CM, Clemons P, & al. e (1983) Insulin antibodies in insulin-dependent
586 diabetics before insulin treatment. *Science* 222:1337.
587 14. Harrison LC (2021) The dark side of insulin: A primary autoantigen and instrument of self-
588 destruction in type 1 diabetes. *Mol Metab*:101288.
589 15. Steck AK*, et al.* (2011) Age of islet autoantibody appearance and mean levels of insulin,
590 but not GAD or IA-2 autoantibodies, predict age of diagnosis of type 1 diabetes: diabetes
591 autoimmunity study in the young. *Diabetes Care* 34(6):1397-1399.
592 16. Michels AW*, et al.* (2017) Islet-Derived CD4 T Cells Targeting Proinsulin in Human
593 Autoimmune Diabetes. *Diabetes* 66(3):722-734.
594 17. Nakayama M*, et al.* (2015) Regulatory vs. inflammatory cytokine T-cell responses to
595 mutated insulin peptides in healthy and type 1 diabetic subjects. *Proc Natl Acad Sci U S A*
596 112(14):4429-4434.
597 18. Yang J*, et al.* (2014) Autoreactive T cells specific for insulin B:11-23 recognize a low-
598 affinity peptide register in human subjects with autoimmune diabetes. *Proc Natl Acad Sci*
599 *U S A* 111(41):14840-14845.
600 19. Cusick MF, Libbey JE, & Fujinami RS (2012) Molecular mimicry as a mechanism of
601 autoimmune disease. *Clin Rev Allergy Immunol* 42(1):102-111.
602 20. Stadinski BD*, et al.* (2010) Diabetogenic T cells recognize insulin bound to IAg7 in an
603 unexpected, weakly binding register. *Proc Natl Acad Sci U S A* 107(24):10978-10983.
604 21. Sakamoto M & Benno Y (2006) Reclassification of Bacteroides distasonis, Bacteroides
605 goldsteinii and Bacteroides merdae as Parabacteroides distasonis gen. nov., comb. nov.,

606 Parabacteroides goldsteinii comb. nov. and Parabacteroides merdae comb. nov. *Int J Syst*
607 *Evol Microbiol* 56(Pt 7):1599-1605.
608 22. Wan X*, et al.* (2018) Pancreatic islets communicate with lymphoid tissues via exocytosis
609 of insulin peptides. *Nature* 560(7716):107-111.
610 23. Sofi MH*, et al.* (2019) Polysaccharide A-Dependent Opposing Effects of Mucosal and
611 Systemic Exposures to Human Gut Commensal Bacteroides fragilis in Type 1 Diabetes.
612 *Diabetes* 68(10):1975-1989.
613 24. Fuchtenbusch M, Larger E, Thebault K, & Boitard C (2005) Transfer of diabetes from
614 prediabetic NOD mice to NOD-SCID/SCID mice: association with pancreatic insulin
615 content. *Horm Metab Res* 37(2):63-67.
616 25. Tang Q*, et al.* (2004) In vitro-expanded antigen-specific regulatory T cells suppress
617 autoimmune diabetes. *J Exp Med* 199(11):1455-1465.
618 26. Liu T, Soong L, Liu G, Konig R, & Chopra AK (2009) CD44 expression positively
619 correlates with Foxp3 expression and suppressive function of CD4+ Treg cells. *Biol Direct*
620 4:40.
621 27. Saxena V, Ondr JK, Magnusen AF, Munn DH, & Katz JD (2007) The countervailing
622 actions of myeloid and plasmacytoid dendritic cells control autoimmune diabetes in the
623 nonobese diabetic mouse. *J Immunol* 179(8):5041-5053.
624 28. Carrero JA*, et al.* (2017) Resident macrophages of pancreatic islets have a seminal role in
625 the initiation of autoimmune diabetes of NOD mice. *Proc Natl Acad Sci U S A*
626 114(48):E10418-E10427.
627 29. Klementowicz JE*, et al.* (2017) Cutting Edge: Origins, Recruitment, and Regulation of
628 CD11c(+) Cells in Inflamed Islets of Autoimmune Diabetes Mice. *J Immunol* 199(1):27-
629 32.
630 30. Vatanen T*, et al.* (2018) The human gut microbiome in early-onset type 1 diabetes from
631 the TEDDY study. *Nature* 562(7728):589-594.
632 31. Wang Y*, et al.* (2018) C-terminal modification of the insulin B:11-23 peptide creates
633 superagonists in mouse and human type 1 diabetes. *Proc Natl Acad Sci U S A* 115(1):162-
634 167.
635 32. Mason D (1998) A very high level of crossreactivity is an essential feature of the T-cell
636 receptor. *Immunol Today* 19(9):395-404.
637 33. Calis JJ, de Boer RJ, & Kesmir C (2012) Degenerate T-cell recognition of peptides on
638 MHC molecules creates large holes in the T-cell repertoire. *PLoS Comput Biol*
639 8(3):e1002412.
640 34. Wucherpfennig KW & Strominger JL (1995) Molecular mimicry in T cell-mediated
641 autoimmunity: viral peptides activate human T cell clones specific for myelin basic protein.
642 *Cell* 80(5):695-705.
643 35. Mana P*, et al.* (2004) Tolerance induction by molecular mimicry: prevention and
644 suppression of experimental autoimmune encephalomyelitis with the milk protein
645 butyrophilin. *Int Immunol* 16(3):489-499.
646 36. Tian J, Lehmann PV, & Kaufman DL (1994) T cell cross-reactivity between
647 coxsackievirus and glutamate decarboxylase is associated with a murine diabetes
648 susceptibility allele. *J Exp Med* 180(5):1979-1984.
649 37. Atkinson MA*, et al.* (1994) Cellular immunity to a determinant common to glutamate
650 decarboxylase and coxsackie virus in insulin-dependent diabetes. *J Clin Invest* 94(5):2125-
651 2129.

652 38. Honeyman MC, Stone NL, Falk BA, Nepom G, & Harrison LC (2010) Evidence for
653 molecular mimicry between human T cell epitopes in rotavirus and pancreatic islet
654 autoantigens. *J Immunol* 184(4):2204-2210.
655 39. Wen L*, et al.* (2008) Innate immunity and intestinal microbiota in the development of Type
656 1 diabetes. *Nature* 455(7216):1109-1113.
657 40. Markle JG*, et al.* (2013) Sex differences in the gut microbiome drive hormone-dependent
658 regulation of autoimmunity. *Science* 339(6123):1084-1088.
659 41. Sun J*, et al.* (2015) Pancreatic beta-Cells Limit Autoimmune Diabetes via an
660 Immunoregulatory Antimicrobial Peptide Expressed under the Influence of the Gut
661 Microbiota. *Immunity* 43(2):304-317.
662 42. Kriegel MA*, et al.* (2011) Naturally transmitted segmented filamentous bacteria segregate
663 with diabetes protection in nonobese diabetic mice. *Proc Natl Acad Sci U S A*
664 108(28):11548-11553.
665 43. Hanninen A*, et al.* (2018) Akkermansia muciniphila induces gut microbiota remodelling
666 and controls islet autoimmunity in NOD mice. *Gut* 67(8):1445-1453.
667 44. Atkinson MA, Roep BO, Posgai A, Wheeler DCS, & Peakman M (2019) The challenge of
668 modulating beta-cell autoimmunity in type 1 diabetes. *Lancet Diabetes Endocrinol*
669 7(1):52-64.
670 45. Roep BO, Atkinson M, & von Herrath M (2004) Satisfaction (not) guaranteed: re-
671 evaluating the use of animal models of type 1 diabetes. *Nat Rev Immunol* 4(12):989-997.
672 46. Skyler JS (2018) Hope vs hype: where are we in type 1 diabetes? *Diabetologia* 61(3):509-
673 516.
674 47. Al-Sakkaf L*, et al.* (1989) Persistent reduction of CD4/CD8 lymphocyte ratio and cell
675 activation before the onset of type 1 (insulin-dependent) diabetes. *Diabetologia* 32(5):322-
676 325.
677 48. Wong FS*, et al.* (2009) Activation of insulin-reactive CD8 T-cells for development of
678 autoimmune diabetes. *Diabetes* 58(5):1156-1164.
679 49. Wong FS*, et al.* (1999) Identification of an MHC class I-restricted autoantigen in type 1
680 diabetes by screening an organ-specific cDNA library. *Nat Med* 5(9):1026-1031.
681 50. Viisanen T*, et al.* (2019) FOXP3+ Regulatory T Cell Compartment Is Altered in Children
682 With Newly Diagnosed Type 1 Diabetes but Not in Autoantibody-Positive at-Risk
683 Children. *Front Immunol* 10:19.
684 51. Grinberg-Bleyer Y*, et al.* (2010) IL-2 reverses established type 1 diabetes in NOD mice by
685 a local effect on pancreatic regulatory T cells. *J Exp Med* 207(9):1871-1878.
686 52. Maruvada P, Leone V, Kaplan LM, & Chang EB (2017) The Human Microbiome and
687 Obesity: Moving beyond Associations. *Cell Host Microbe* 22(5):589-599.
688 53. Rinaldi M, Perricone R, Blank M, Perricone C, & Shoenfeld Y (2013) Anti-Saccharomyces
689 cerevisiae autoantibodies in autoimmune diseases: from bread baking to autoimmunity.
690 *Clin Rev Allergy Immunol* 45(2):152-161.
691 54. Gevers D*, et al.* (2014) The treatment-naive microbiome in new-onset Crohn's disease. *Cell*
692 *Host Microbe* 15(3):382-392.
693 55. Lamps LW*, et al.* (2003) Pathogenic Yersinia DNA is detected in bowel and mesenteric
694 lymph nodes from patients with Crohn's disease. *Am J Surg Pathol* 27(2):220-227.
695 56. Chassaing B*, et al.* (2011) Crohn disease--associated adherent-invasive E. coli bacteria
696 target mouse and human Peyer's patches via long polar fimbriae. *J Clin Invest* 121(3):966-
697 975.

698 57. Carding S, Verbeke K, Vipond DT, Corfe BM, & Owen LJ (2015) Dysbiosis of the gut
699 microbiota in disease. *Microb Ecol Health Dis* 26:26191.
700 58. Frank DN, *et al.* (2007) Molecular-phylogenetic characterization of microbial community
701 imbalances in human inflammatory bowel diseases. *Proc Natl Acad Sci U S A*
702 104(34):13780-13785.
703 59. Navaneethan U, Venkatesh PG, & Shen B (2010) Clostridium difficile infection and
704 inflammatory bowel disease: understanding the evolving relationship. *World J*
705 *Gastroenterol* 16(39):4892-4904.
706 60. Quagliariello A, *et al.* (2016) Effect of Bifidobacterium breve on the Intestinal Microbiota
707 of Coeliac Children on a Gluten Free Diet: A Pilot Study. *Nutrients* 8(10).
708 61. Vatanen T, *et al.* (2016) Variation in Microbiome LPS Immunogenicity Contributes to
709 Autoimmunity in Humans. *Cell* 165(6):1551.
710 62. Stewart CJ, *et al.* (2018) Temporal development of the gut microbiome in early childhood
711 from the TEDDY study. *Nature* 562(7728):583-588.
712 63. Higashide T, *et al.* (2006) T cell epitope mapping study with insulin overlapping peptides
713 using ELISPOT assay in Japanese children and adolescents with type 1 diabetes. *Pediatr*
714 *Res* 59(3):445-450.
715 64. Kent SC, *et al.* (2005) Expanded T cells from pancreatic lymph nodes of type 1 diabetic
716 subjects recognize an insulin epitope. *Nature* 435(7039):224-228.
717 65. Mannering SI, *et al.* (2005) The insulin A-chain epitope recognized by human T cells is
718 posttranslationally modified. *J Exp Med* 202(9):1191-1197.
719 66. Pathiraja V, *et al.* (2015) Proinsulin-specific, HLA-DQ8, and HLA-DQ8-transdimer-
720 restricted CD4+ T cells infiltrate islets in type 1 diabetes. *Diabetes* 64(1):172-182.
721 67. Mannering SI, Di Carluccio AR, & Elso CM (2019) Neoepitopes: a new take on beta cell
722 autoimmunity in type 1 diabetes. *Diabetologia* 62(3):351-356.
723 68. Delong T, *et al.* (2016) Pathogenic CD4 T cells in type 1 diabetes recognize epitopes
724 formed by peptide fusion. *Science* 351(6274):711-714.
725 69. Kracht MJ, *et al.* (2017) Autoimmunity against a defective ribosomal insulin gene product
726 in type 1 diabetes. *Nat Med* 23(4):501-507.
727 70. Babon JA, *et al.* (2016) Analysis of self-antigen specificity of islet-infiltrating T cells from
728 human donors with type 1 diabetes. *Nat Med* 22(12):1482-1487.
729 71. Tai N, *et al.* (2016) Microbial antigen mimics activate diabetogenic CD8 T cells in NOD
730 mice. *J Exp Med* 213(10):2129-2146.
731 72. Greiling TM, *et al.* (2018) Commensal orthologs of the human autoantigen Ro60 as triggers
732 of autoimmunity in lupus. *Sci Transl Med* 10(434).
733 73. Gil-Cruz C, *et al.* (2019) Microbiota-derived peptide mimics drive lethal inflammatory
734 cardiomyopathy. *Science* 366(6467):881-886.
735 74. Harkiolaki M, *et al.* (2009) T cell-mediated autoimmune disease due to low-affinity
736 crossreactivity to common microbial peptides. *Immunity* 30(3):348-357.
737 75. Dziarski R, Park SY, Kashyap DR, Dowd SE, & Gupta D (2016) Pglyrp-Regulated Gut
738 Microflora Prevotella falsenii, Parabacteroides distasonis and Bacteroides eggerthii
739 Enhance and Alistipes finegoldii Attenuates Colitis in Mice. *PLoS One* 11(1):e0146162.
740 76. Croswell A, Amir E, Teggatz P, Barman M, & Salzman NH (2009) Prolonged impact of
741 antibiotics on intestinal microbial ecology and susceptibility to enteric Salmonella
742 infection. *Infect Immun* 77(7):2741-2753.

77. Chow IT, *et al.* (2019) Discriminative T cell recognition of cross-reactive islet-antigens is associated with HLA-DQ8 transdimer-mediated autoimmune diabetes. *Sci Adv* 5(8):eaaw9336.
78. Mohan JF, *et al.* (2010) Unique autoreactive T cells recognize insulin peptides generated within the islets of Langerhans in autoimmune diabetes. *Nat Immunol* 11(4):350-354.
79. Flodstrom-Tullberg M, *et al.* (2003) Target cell expression of suppressor of cytokine signaling-1 prevents diabetes in the NOD mouse. *Diabetes* 52(11):2696-2700.

FIGURES:

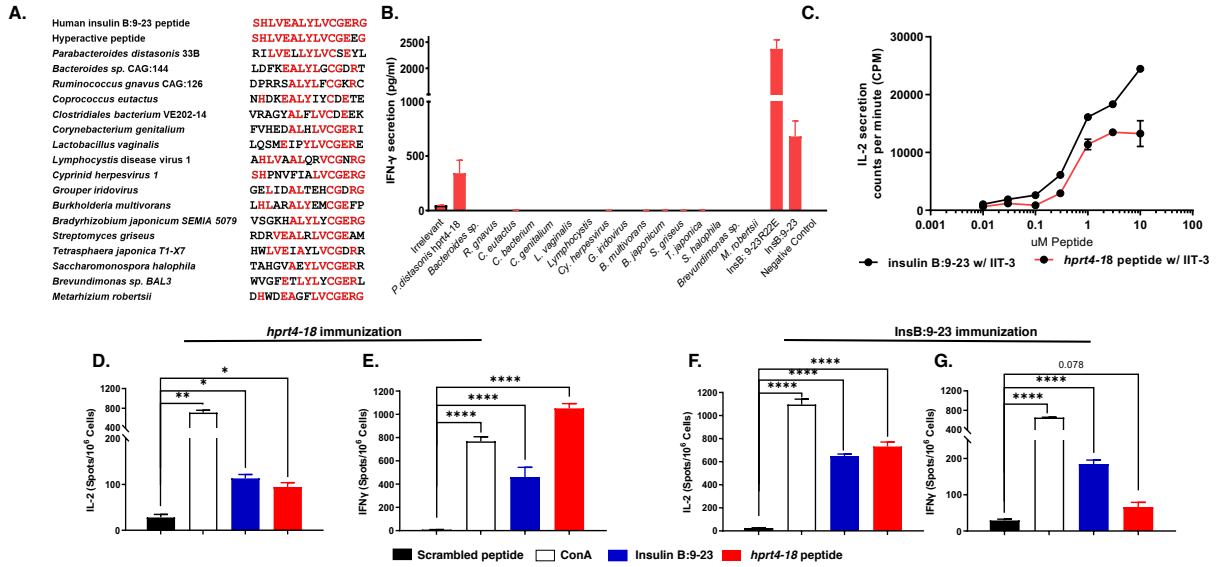

Figure 1. *P. distasonis hprt4-18* peptide mimic can stimulate both human and NOD mice T cells specific to insB:9-23. **(A)** Sequence alignment of 17 microbial peptides tested in this study. The amino acids highlighted in red are identical to insB:9-23. (**B)** Treatment of insB:11-23-specific human T-cell clones with each of selected 17 microbial peptides, where, negative control and irrelevant peptides were used as the negative controls, ins B9-23 and insB:9-23 R^{22E} were used as positive controls. ELISpot was used to determine IFN-γ secretion *(P<0.05)* (n=3). **(C)** Dose response of IIT-3 hybridomas to insB:9-23 (black) or *hpt4-18* peptides to (red) where peptides

761 were presented to hybridomas as covalently linked to I-A^{g7} expressed on macrophages (C3g7
762 cells). Data were presented as IL-2 induced proliferation in CTLL-2 cells. **(D-G)** Mice (n=3/group)
763 were immunized with either *hprt4-18* peptide (**D-E**) or insB:9-23 peptide (**F-G**) after 7 days of
764 immunization, popliteal lymph nodes were stimulated either by *hprt4-18* peptide, insB:9-23, ConA
765 (positive control) or scrambled peptide (negative control). Secretion of IL-2 (**E & G**) and IFN-γ
766 **(D & F)** were determined by ELISpot. All samples in each panel are biologically independent.
767 Data were expressed as means ± SEM. *$P<0.05$, **$P<0.01$, ****$P<0.0001$. Statistical analysis
768 was performed by one-way ANOVA using Dunnett's multiple comparison test.

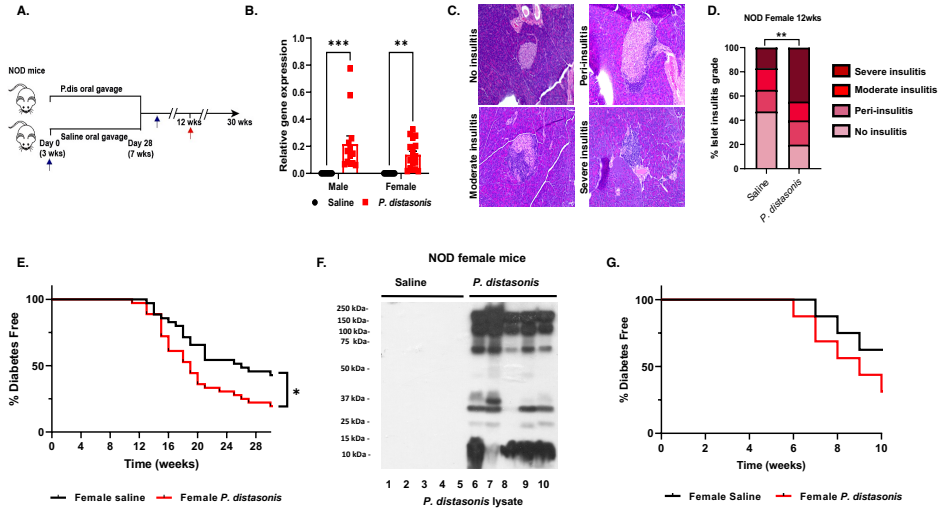

769

770 **Figure 2. *P. distasonis* colonization enhances disease onset in female NOD mice and**
771 **T1D patients have a stronger immune response to *P. distasonis* compared to healthy**
772 **individuals. (A)** Schematic overview of the *P. distasonis* oral gavage experiments
773 (n=40/group/sex). Blue arrow shows the time-point (week 9) of fecal sample collection for qPCR
774 experiments for *P. distasonis* colonization and red arrow shows the time-point (week 12) for
775 pancreata collection for insulitis analysis (n = 5 mice/group/sex). **(B)** Relative abundance of *P.*
776 *distasonis* in fecal samples determined by qPCR (week 12, n=10-13/male, n=12-17/female). **(C)**

777 Representative images of islets insulitis score data where islets were scored as no insulitis, peri-
778 insulitis, moderate insulitis or having severe infiltration as shown in images. **(D)** Quantification of
779 insulitis scores obtained from *P. distasonis* colonized and saline gavaged female NOD mice at
780 week 12 (n=5/group/sex). **(E)** Diabetes incidence in female NOD mice (n=35/group/sex) after
781 daily oral gavage with either saline or *P. distasonis* for four weeks after weaning *(P<0.05)*. **(F)**
782 Western blot analysis performed using serum samples from female NOD mice either oral gavaged
783 with *P. distasonis* or saline (week 12, n=5/group/sex). **(G)** Diabetes incidence of the recipient
784 NOD/SCID mice after adoptive transfer of $5x10^7$ splenocytes/mouse from individual female NOD
785 mice to female NOD/SCID mice at 6 weeks of age (1:1 ratio, same gender, n=15). All samples in
786 each panel are biologically independent. Log-rank (Mantel-cox) test was used for survival curves
787 and adoptive transfer experiment. Data were expressed as mean ± SEM. **P<0.05*, ***P<0.01*,
788 ****P<0.01*. Statistical analysis was performed by two-way ANOVA using Sídak multiple
789 comparison test or two-tailed unpaired Student's *t*-test.

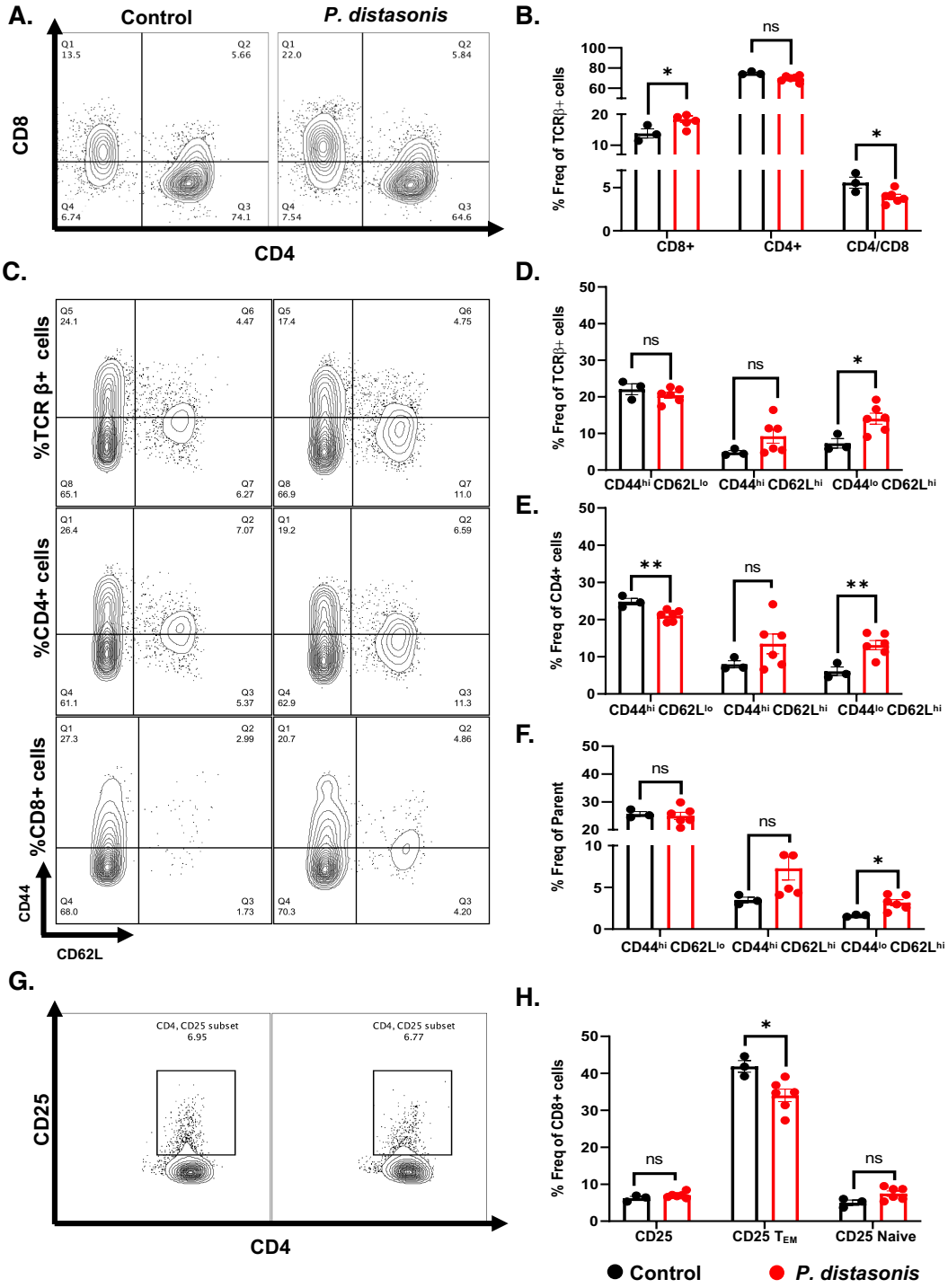
A.
Control
P. distasonis
CD8
CD4
Q1 13.5
Q2 5.66
Q4 6.74
Q3 74.1
Q1 22.0
Q2 5.84
Q4 7.54
Q3 64.6
B.
% Freq of TCRβ+ cells
ns
*
*
CD8+
CD4+
CD4/CD8
C.
%TCR β+ cells
%CD4+ cells
%CD8+ cells
CD44
CD62L
Q5 24.1
Q6 4.47
Q8 65.1
Q7 6.27
Q5 17.4
Q6 4.75
Q8 66.9
Q7 11.0
Q1 26.4
Q2 7.07
Q4 61.1
Q3 5.37
Q1 19.2
Q2 6.59
Q4 62.9
Q3 11.3
Q1 27.3
Q2 2.99
Q4 68.0
Q3 1.73
Q1 20.7
Q2 4.86
Q4 70.3
Q3 4.20
D.
% Freq of TCRβ+ cells
ns
ns
*
CD44hi CD62Llo
CD44hi CD62Lhi
CD44lo CD62Lhi
E.
% Freq of CD4+ cells
**
ns
**
CD44hi CD62Llo
CD44hi CD62Lhi
CD44lo CD62Lhi
F.
% Freq of Parent
ns
ns
*
CD44hi CD62Llo
CD44hi CD62Lhi
CD44lo CD62Lhi
G.
CD25
CD4
CD4, CD25 subset 6.95
CD4, CD25 subset 6.77
H.
% Freq of CD8+ cells
*
ns
ns
CD25
CD25 TEM
CD25 Naive
Control
P. distasonis

790

791 **Figure 3: *P. distasonis* colonization increase CD8+ T-cells and Naïve cells phenotype**.
792 Mice were orally gavaged with either *P. distasonis* or saline for 4-weeks after weaning and
793 analyzed at 12 weeks of age. **(A)** Representative image from a single experimental cohort of FACS
794 analyses for splenic CD4+ and CD8+ T-cells from saline and *P. distasonis* gavaged mice. **(B)**
795 CD4+ and CD8+ cells as percent of TCR-β+ immune cell subsets and ratio of splenic CD4+ to
796 CD8+ T-cells. **(C)** $CD44^{lo/hi}$ and $CD62L^{lo/hi}$ T-cells in TCR-β+, CD4+ and CD8+ T-cells. **(D)**
797 Percent of $CD44^{hi}$ $CD62L^{lo}$ (T_{EM})**,** $CD44^{hi}$ $CD62L^{hi}$ (T_{CM})**,** $CD44^{lo}$ $CD62L^{hi}$ (Naive) in TCR-β^{+}
798 immune cell subsets, **(E)** Percent of $CD44^{hi}$ $CD62L^{lo}$ (T_{EM})**,** $CD44^{hi}$ $CD62L^{hi}$ (T_{CM})**,** $CD44^{lo}$
799 $CD62L^{hi}$ (Naive) in CD4+ immune T-cell subsets; **(F)** Percent of $CD44^{hi}$ $CD62L^{lo}$ (T_{EM})**,** $CD44^{hi}$
800 $CD62L^{hi}$ (T_{CM})**,** $CD44^{lo}$ $CD62L^{hi}$ (Naive) in CD8+ immune T-cell subsets **(G)** Representative
801 image of FACS analyses of CD4+, CD25+ Treg population in saline and *P. distasonis* gavaged
802 mice. **(H)** Percent of CD4+ CD25+ cells in CD4+ single cell subsets**,** $CD44^{hi}$ $CD62L^{lo}$ (T_{EM}) and
803 $CD44^{lo}$ $CD62L^{hi}$ (Naive) population in percent of CD4+ CD25+ single cell subsets. All samples
804 in each panel are biologically independent. Spleens were obtained from female NOD mice oral
805 gavaged with either *P. distasonis* (n=6) or saline (n=3). Data were expressed as means ± SEM. *,
806 $P<0.05$, **, $P<0.01$, ***, $P<0.001$. Statistical analysis was performed by two-tailed, unpaired
807 Student's t-test.

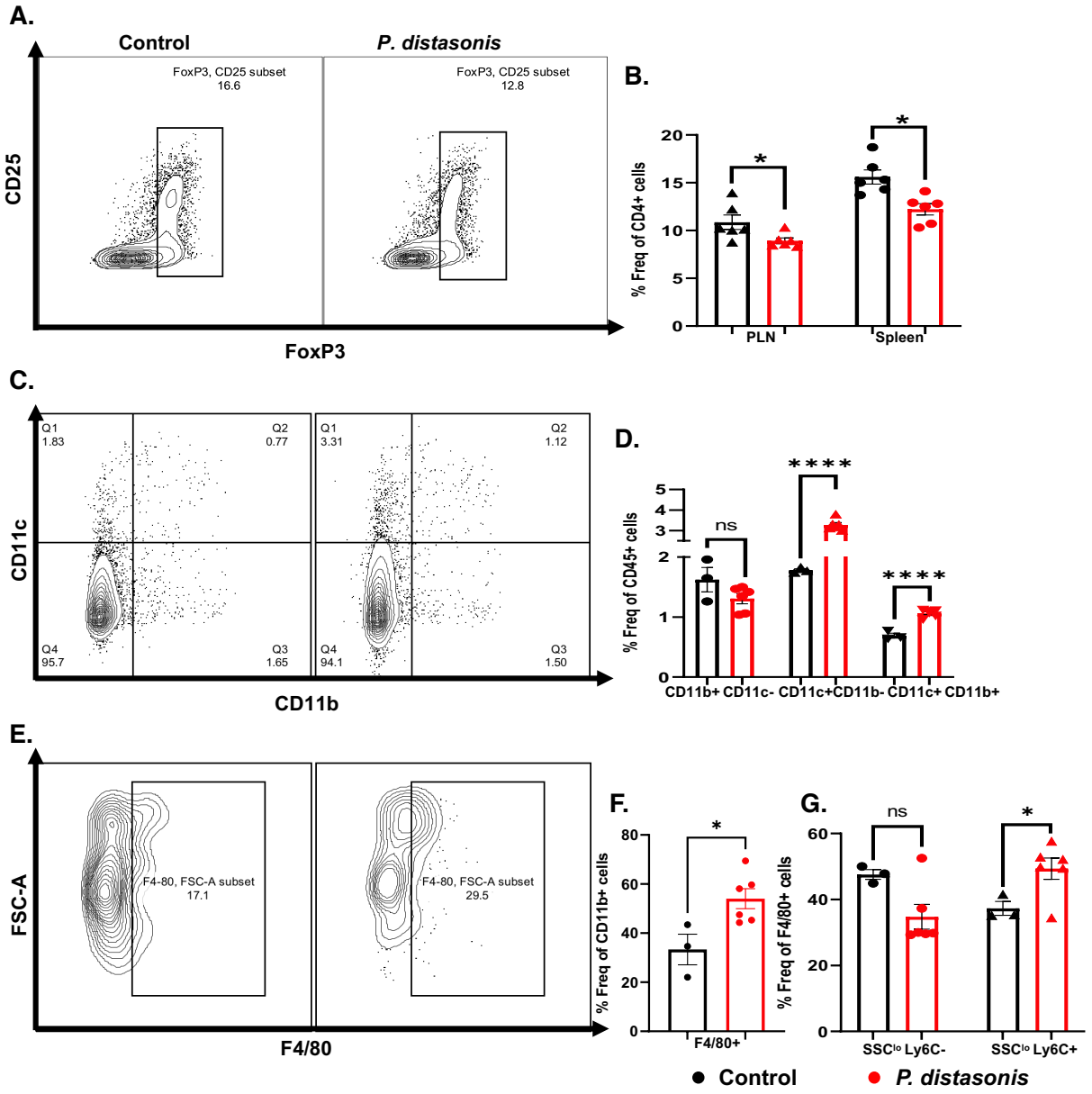

Figure 4: *P. distasonis* colonization decreases Foxp3+ cells and increases dendritic, and macrophage populations. **(A)** Representative image of FACS analyses of splenic Foxp3+ cells in saline and *P. distasonis* gavaged mice. **(B)** Percent of Foxp3+ cells in CD4+ T-cell subsets. **(C)** Representative image of FACS analyses of dendritic cells (CD11b-CD11c+ and CD11c+ CD11b+) in saline and *P. distasonis* gavaged mice. **(D)** Percent of CD11b+/-CD11c+/- population in splenic single cell subsets **(E)** Representative image of FACS analyses of macrophages

815 (F4/80+cells) in spleen of saline and *P. distasonis* gavaged mice. **(F)** Percent of F4/80+ cells in
816 CD11b+ cell subsets **(G)** Percent of F4/80+ cell subsets, where $SSC^{lo}Ly6C^{lo}$ represents residential
817 macrophage and $SSC^{lo}Ly6C^{hi}$ represents circulatory macrophages. All samples in each panel are
818 biologically independent. Spleens were obtained from female NOD mice oral gavaged with either
819 *P. distasonis* (n=6) or saline (n=3). Data were expressed as means ± SEM. *, $P<0.05$, **, $P<0.01$,
820 ***, $P<0.001$. Statistical analysis was performed by two-tailed, unpaired Student's t-test.

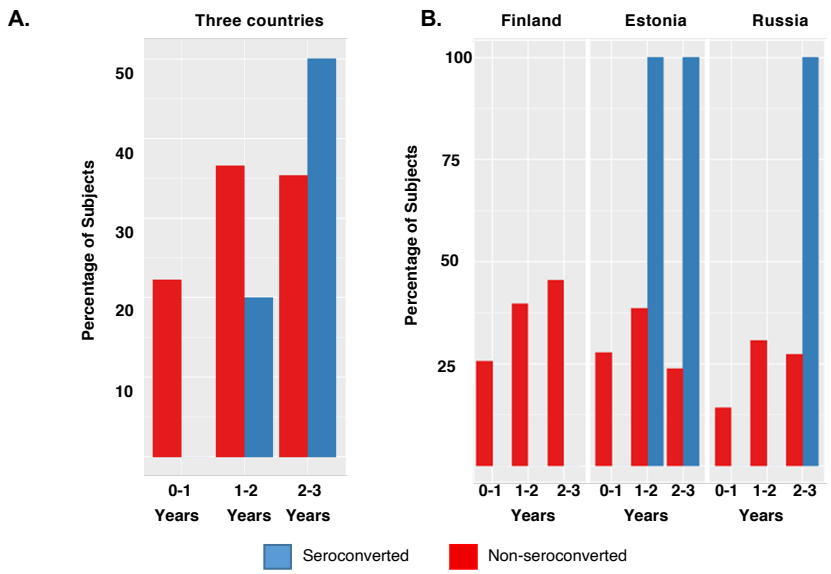

821

822 **Figure 5. Reanalysis of DIABIMMUNE gut microbiome data revealed the presence**
823 **of sequences encoding *P. distasonis hprt4-18* peptide in all children developing autoantibodies**
824 **in Estonia after age 1 and Russia after age 2 (A-B)** Reanalysis of DIABIMMUNE gut
825 microbiome data for the presence of *hprt4-18* peptide **(A)** The percentage of subjects having
826 sequence encoding *hprt4-18* in the gut in all three countries (Finland, Estonia and Russia) and **(B)**
827 in individual countries at different phases of gut microbiota development (age 0 to 3). Blue
828 represents subjects that developed autoantibodies (seroconverted) and red represents subjects with

829 no autoantibodies (non-seroconverted). 16 of 74 subjects in Finland, 14 of 74 of subjects in
830 Estonia, 4 of 74 subjects in Russia developed autoantibodies during the study.

831

832